

## Identification of Nomex<sup>®</sup> Honeycomb Cores Mechanical Properties and Failure Criteria Based on Experimental and Numerical Approaches

Laurent Gornet<sup>1</sup>, Gilles Marckmann, Steven Marguet, Syed Kamran-Ali

### Summary

The mechanical properties of Nomex<sup>®</sup> honeycomb cores are determined through a combined experimental and numerical approach. The proposed method relies on out-of-plane shear tests on four blocks specimens and on standard ASTM compressive tests. These mechanical tests are designed and analyzed thanks to finite elements simulations involving randomly distributed geometric defects and failures due to instabilities. The full three-dimensional mechanical properties of Nomex<sup>®</sup> honeycomb cores are then computed with the prototype software NidaCore by inverse scaling of the mechanical properties of the constitutive Nomex<sup>®</sup> paper on available experimental data. Moreover, the failure envelope of Nomex<sup>®</sup> cores are predicted by the use of a coupled approach involving experimental results and numerical simulations and based on the understanding of local instability mechanisms. A failure criterion is then proposed.

**keywords:** Nomex<sup>®</sup> honeycomb cores, homogenization, finite elements modelling, compression testing, shear testing.

### Introduction

The purpose of this study is to enhance the understanding and modelling of the mechanical behaviour of Nomex<sup>®</sup> honeycomb cores. Associated with carbon/epoxy laminates, these materials form sandwich structures which are widely used in the manufacturing of transoceanic sailing race boats (Gornet *et al* 2006).

The mechanical behaviour of the different elementary materials constituting the sailing boat must be investigated in order to integrate the experimental data of materials in finite elements simulations as soon as the design process starts (Martin *et al* 2006). Experimental as well as numerical approaches are used to determine the three-dimensional mechanical behaviour of the Nomex<sup>®</sup> honeycomb cores under quasi-static condition. The collapse of hexagonal (ECA-H) and rectangular (ECA-R) honeycomb cores is related to the phenomenon of loss of stability (Gibson L.J., Ashby M.F., 1988). It is due to the local buckling of the cell walls (Gornet *et al* 2004), and results in a full deterioration of the cores. The catalogue of Nomex<sup>®</sup> cores of Hexcel (1999) points out that “Users should make their own assessment of the suitability of any product for the purposes required”, and Euro-Composite (1999) states that “Data is based on results gained from experience and tests and

---

<sup>1</sup>École Centrale Nantes, GeM UMR-CNRS 6183, 1 rue de la Noë, BP 92101, 44321 Nantes Cedex 3, France, Tel. (33)2 40 37 25 82, Fax. (33)2 40 37 25 73, E-mail. laurent.gornet@ec-nantes.fr

is believed to be accurate yet without acceptance of liability for loss or damage incurred and attributable to reliance thereon as conditions of use lie outside our control”.

Consequently, the Nomex<sup>®</sup> cores must be validated by the designers of structures in order to check their designs in a pertinent way.

In this study, the characterization of the three-dimensional mechanical behaviour of the Nomex<sup>®</sup> honeycomb cores is carried out using an experimental work coupled with finite elements simulations. Three-dimensional mechanical properties of the Nomex<sup>®</sup> cores are inferred from simulations using the prototype software NidaCore. This software has been developed in laboratory and is based on finite elements code Cat3M-CEA (Gornet *et al* 2004). Initial simulations have been validated using the catalogues of the manufacturers, Hexcel and Euro-Composite (1999). These numerical results are compared with experimental data obtained from standard out-of-plane compression tests (ASTM C365) and non standard out-of-plane shear tests. The shear test (ASTM C273), commonly used by the manufacturers of Nomex<sup>®</sup> to characterize their materials, does not produce a pure shear stress state. As a consequence, choice was made to use a test-sample containing four blocks of Nomex<sup>®</sup> honeycombs to ensure pure shear kinematics. The geometry of the test-sample has been determined using many finite elements simulations which have highlighted the importance of scale effects on the material parameters obtained. Experiments have confirmed numerical predictions and the quality of the proposed four blocks shear test. Moreover, the mechanical elastic behaviour as well as the ultimate stresses under complex loading conditions have been numerically determined from the software NidaCore (Gornet *et al* 2006). This software is based on the theories of periodic homogenization and elastic instability applied on a Representative Volume Element. The RVE of the honeycombs involves three orthogonal planes of symmetry, which lead to an orthotropic equivalent medium.

The finite elements simulations carried out using the NidaCore code do not only allow to minimize the experimental work but make it also possible to define the rupture stress envelopes under the action of complex mechanical conditions that lead to instability. The mechanism of rupture by buckling is clearly elaborated in the literature (Gibson and Ashby 1988, Zhang J., M.F. Ashby 1992, Petras and Sutcliffe, 1999, 2000, Aminanda *et al* 2005, Gornet *et al* 2004, 2006). The relevance of the theoretical approach, suggested to compute the envelope of rupture, is confirmed by the experimental results generated by the ARCAN test presented by (Petras and Sutcliffe, 2000).

### **Experiments**

A great number of mechanical tests, standardized or not, is proposed in the literature to characterize the mechanical behaviour of the honeycomb cores: the test

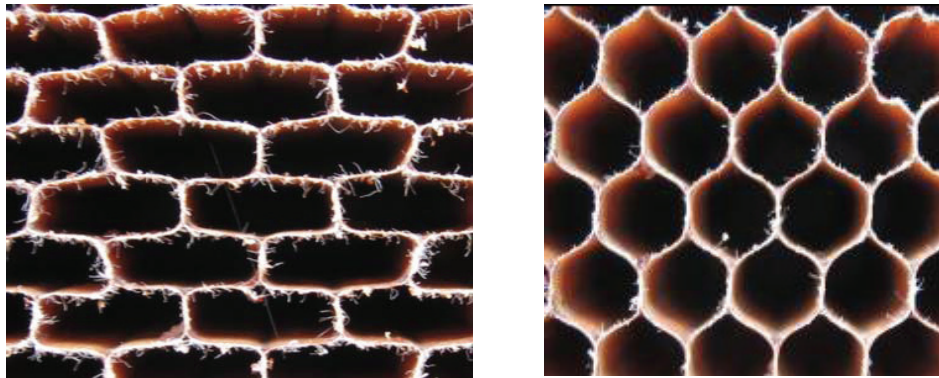


Figure 1: ECA-H and ECA-R 6,4 mm  $64 \text{ kg.m}^{-3}$  Nomex<sup>®</sup> geometries

of delamination of walls (ASTM C362), the test of compression (ASTM C365), the one block diagonal shear test (ASTM C273), the test of combined compression and shear (ARCAN), or, the test of inflection on sandwich (ASTM C393). In this study, a canonical base of three mechanical tests associated to finite elements simulations is proposed to determine all the quasi-static three-dimensional mechanical properties of Nomex<sup>®</sup> honeycomb cores (Hexcel 1999, Euro-Composite 1999).

The proposed approach relies on a test-sample for pure out-of-plane shear in L direction, a test-sample for pure out-of-plane shear in W direction and on a test-sample for standardized out-of-plane compression, ASTM (ASTM C365).

The presented tests have made it possible to characterize the mechanical behaviour of two types of Nomex<sup>®</sup> honeycomb cores visible on figure 1. In order to check the influence of the height of the block on the mechanical properties, experimental investigations have been performed on hexagonal honeycombs ECA-H of height 12.7 mm and diameter 6.4 mm and on rectangular over-expanded ones ECA-R of height 40 mm and diameter 6.4 mm. These two materials have the same density of  $64 \text{ kg.m}^{-3}$ . The tests have been carried out on a hydraulic tensile testing machine MTS of 25 kN of strength capacity.

The mechanical properties measured at the end of the experimental phase are: the modulus of out-of-plane compression ( $E_T$  or  $E_{33}$ ), the deformation with instability, the two out-of-plane shear moduli ( $G_L$  and  $G_W$  or  $G_{13}$  and  $G_{23}$ ) as well as the two associated stresses and deformations of rupture. During the mechanical tests, the presence of a scale effect was highlighted by the use of several sizes of test-samples, in agreement with the previous numerical simulations.

#### **Out-of-plane compression test**

The out-of-plane compression tests proposed in (ASTM C365) allows the determination of the modulus of compression ( $E_{33}$ ) and its associated rupture stress ( $\sigma_{33c}$ ). The shapes of a test-sample of 40 mm height are presented during and after

compression in figure 2.

The specimens are placed between two plates of compression and crushed up to a maximum strain of 90 % with an imposed velocity of  $0.025 \text{ mm.s}^{-1}$ . The associated compressive quasi-static strain rate is  $1.10^{-3} \text{ s}^{-1}$ . Two stress versus strain curves are plotted on figure 3 for these quasi-static conditions and several other curves are plotted for higher strain rates. They all show the existence of three major crushing steps. The first one, a linear growth of the stress versus strain, is related to the reversible elastic response of the Nomex<sup>®</sup> honeycomb core. Once a critical load is reached, corresponding to a compressive stress of roughly 3.6 MPa, a brutal decrease in stress is observed. This phenomenon is in link with the apparition of a global instability within the honeycomb core. It is due to the local buckling of the walls of the honeycombs, local buckling that gather to form a global mode of instability (figure 2). After this first global collapse of the structure, a slightly rising plateau is observed, before a ultimate phase of densification, traduced by the increase in stress and due to the accumulation of crushed material between the skins.

It can be noticed here that the stress versus strain curves are very similar which proves the data to be reliable and that no strain rate effect occurs. The experimental data and predictions are presented in table 1.

Table 1: Comparison between computed values and experimental data (ECA-R)

	$E_{33}$ (MPa)	$\sigma_{33c}$ (MPa)
Experimental	155	3.6
Computed	180	4.1

In Hexcel's catalogue, there is no data for thicknesses different from 12.7 mm. This demonstrates all the interest to have a reliable predictive method to determine full three-dimensional mechanical properties of Nomex<sup>®</sup> cores. However, to give an order of comparison, the Young's modulus and the crushing stress for a Nomex<sup>®</sup> honeycomb core of thickness 12.7 mm are equal to 255 MPa and 4.5 MPa respectively. Hence, the values obtained from the crushing tests seem to be coherent with the fact that when the thickness of the core goes up, the mechanical properties decrease (Young's modulus and crushing strength).

#### **Out-of-plane shear test**

The out-of-plane shear tests are elaborated using four blocks test-samples ensuring a pure kinematics of shear for each of the four blocks (figure 4). These tests make it possible to measure the two out-of-plane moduli of rigidity ( $G_L$  and  $G_W$ ). The stress deformation curves established from the shear tests are presented on figure 5.



Figure 2: Shapes of failure of an ECA-R specimen during and after compressive loading

#### **Scale effect in out-of-plane shear**

The presence of a scale effect has been experimentally checked on shear test-samples of Nomex® ECA-R 40 mm, 6,4 mm, 64 kg.m<sup>-3</sup>. The sheared blocks were cut down successively by 1/7 th; 2/7 th; 3/7 th; 4/7 th; 5/7 th and 6/7 th of their initial surface. The evolution of the measured shear modulus in experiments is presented on figure 6.

#### **Simulation of the Edge Effect**

In this part, finite elements simulations carried out on an arrangement of cells modelled by shell elements enable to determine the dependence of the out-of-plane shear modulus on geometrical parameters. Simulations have been conducted under the assumption of linear elasticity with small perturbations for heights of cores equal to 4; 12.7; 40 and 90 mm. The length of the virtual test-sample has been taken equal to 2; 4; 8; 12; 24; 48; or 96 cells. A distribution of the stored energy is presented in figure 7 for the model involving 12 cells. The edge effect clearly appears, there is less stored energy near the edge than in the centre of the specimen

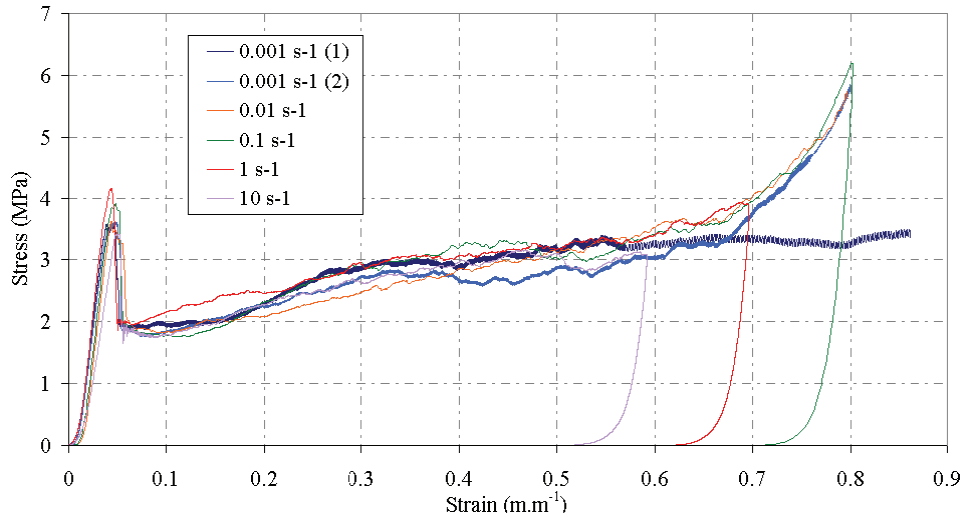


Figure 3: ECA-R under compressive loadings ( $E_{33}$ ), stress versus strain curve

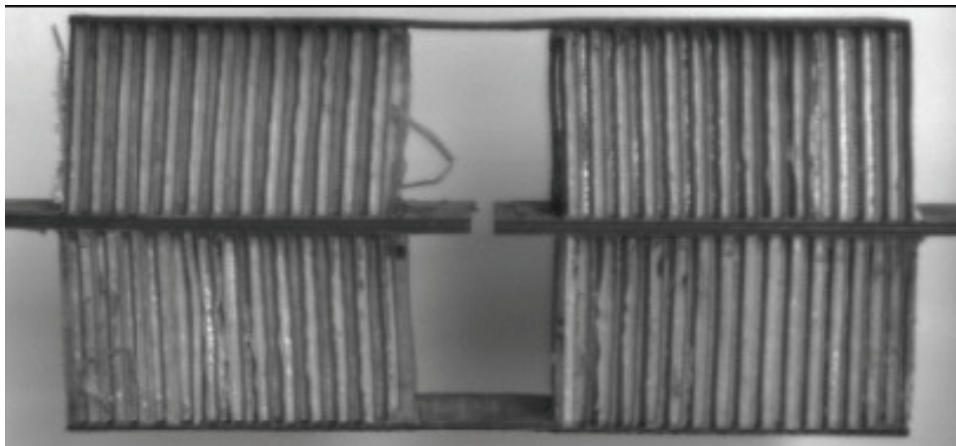


Figure 4: Four blocks shear sample, deformed configuration, ECA-R ( $E_L$ )

(see figure 9 for an illustration of the repartition of the stored energy per cell). This leads to a scale effect affecting the measured properties of the test-sample.

Figure 8 shows that for a given height of block, the identified shear modulus tends asymptotically towards its stabilized value when the number of cells increases. In the case of the proposed four blocks test-sample, the length of blocks must be of at least 127,2 mm in the L direction and 157,2 mm in the W direction. Standard norm ASTM C273-94 recommends a block length equal to 12 times the height of the core for its test, which corresponds, in the presented case, to a length of 152,4 mm. For a standardized height of block of 12,7mm (ASTM C273-94), it

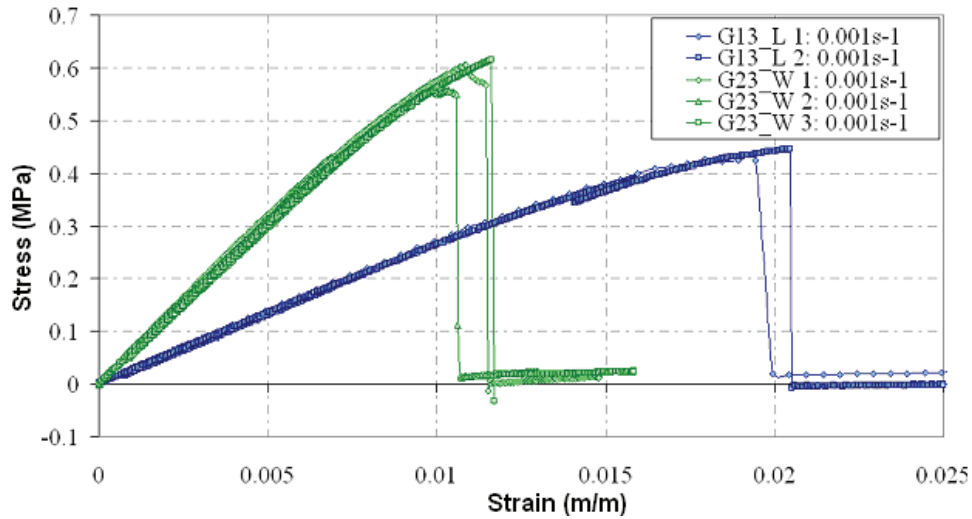


Figure 5: Nomex<sup>®</sup> ECA-R, 40 mm, shear tests

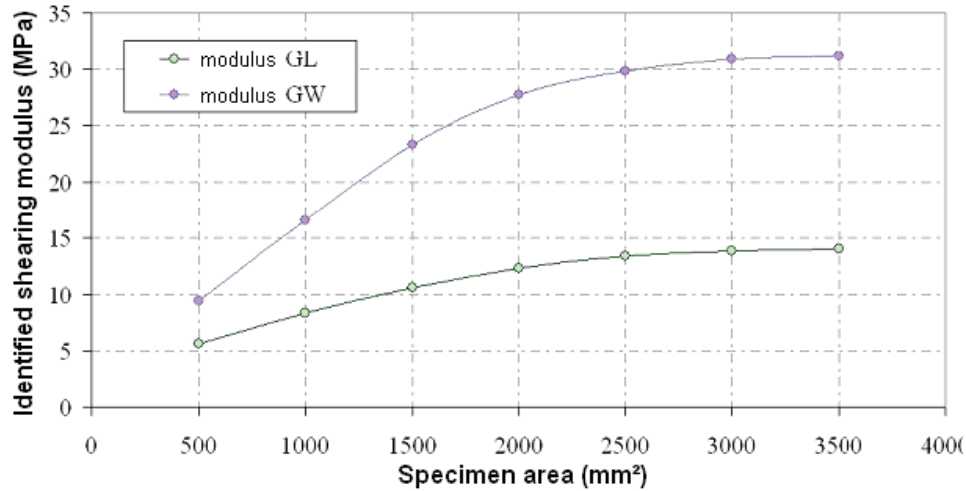


Figure 6: Evolution of shear modulus versus block shear surface for ECA-R

seems necessary to take into account at least 24 cells in direction of shear to obtain a stabilized shear modulus (figures 8 and 9).

### Virtual-Sample Program

A “virtual sample”, entirely parameterized and made of several cells meshed by shell elements, has been developed using the finite elements code Cast3M in order to validate the relevance of the experimental results. This virtual sample can be solicited in out-of-plane compression and/or shear. An internal examination area can be inspected in order to validate the length of penetration of edge effects in the

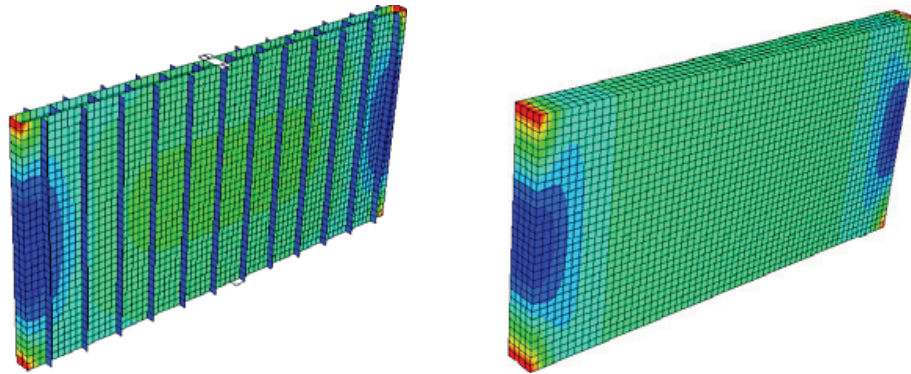


Figure 7: Energy distribution for discrete ECA-R and homogeneous equivalent body under shear loading

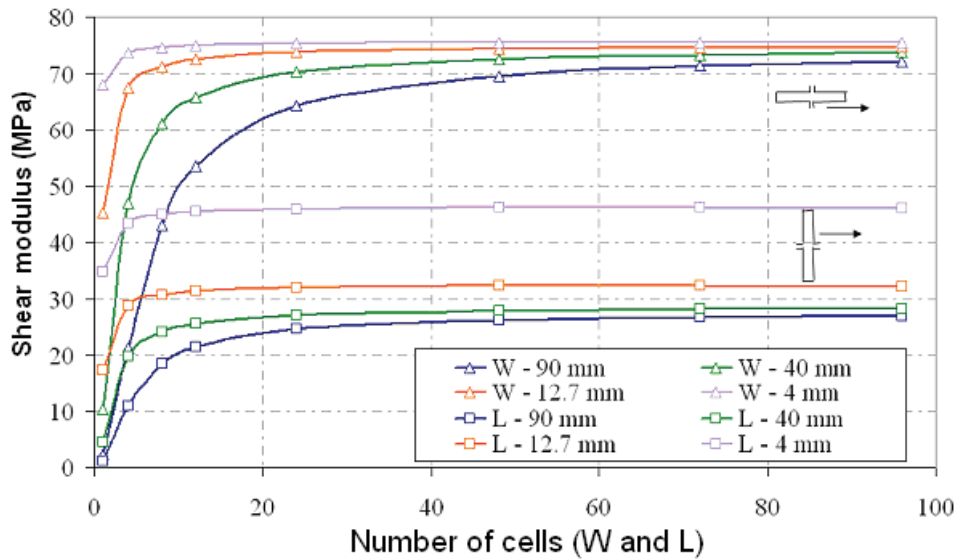


Figure 8: Shear modulus versus number of Nomex<sup>®</sup> cells for ECA-R

block of Nomex<sup>®</sup> honeycombs. The influence of the area of edge effect can thus be evaluated numerically from the calculation of the energy of deformation. Moreover, geometrical imperfections can be generated on the cells of the honeycombs using a Gaussian noise (figures 10 and 11). The research of buckling modes allows the determination of the ultimate stresses as was done before. The geometrical defects introduce a multitude of modes of instability of close values. The computation of the mechanical properties without taking into account the edge zone leads to moduli of higher values than if the whole specimen is considered.

The simulations performed confirm the experimental results.

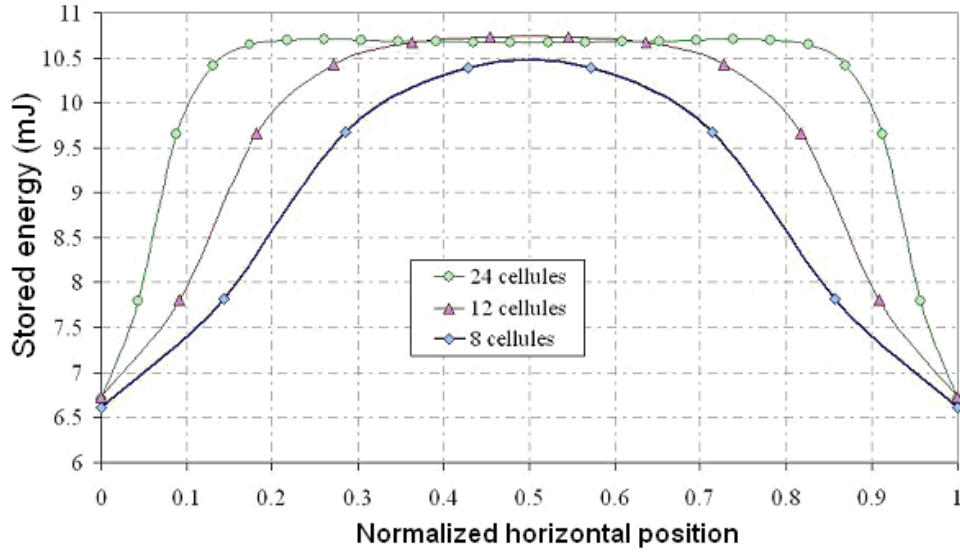


Figure 9: Energy distribution for ECA-R under shearing loading

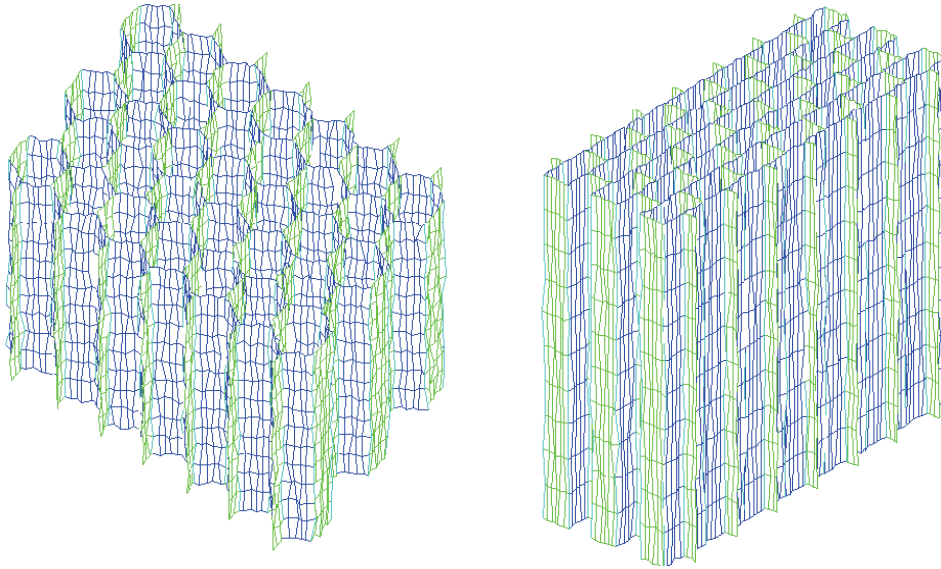


Figure 10: Virtual specimens with randomly distributed defects

### Theoretical Aspects of Nidacore Software

This prototype software relies on the theory of the homogenization of periodic media. It is developed using the process control language Gibiane of the finite elements code Cast3M CEA (Gornet *et al* 2004). Mechanical characteristics of Nomex<sup>®</sup> paper used in the model are determined backwards by inverse scaling of

the out-of-plane shear moduli of the homogenized core compared to the experimental results. Out-of-plane moduli  $G_L$  and  $G_W$  and associated stresses of rupture  $\sigma_L$  and  $\sigma_W$  as well as the crushing stress  $\sigma_T$  are the only data usually provided by the manufacturers of honeycomb cores. The second version of prototype software NidaCore make it possible to obtain a more general tool by adding, in the Representative Volume Element, the interaction between the core and the two skins (Gornet *et al* 2006). Moreover, NidaCore is able to compute the ultimate stresses of the RVE and as a consequence, to create the envelope of failure of the studied core.

### General concept

The Representative Volume Elements ( $Y$ ) adopted for the homogenization of the hexagonal and rectangular over-expanded honeycomb cores are presented in figure 11. Any larger volume can be obtained by successive translations of these RVE. The orthotropic basis of the honeycomb cells are  $(e_1, e_2, e_3)$ .

Strain based periodic homogenization rests on the data of an average strain field  $E$  imposed to a RVE and which enables the computation of the compliance. It must be highlighted that for periodic homogenization, stress or strain approaches are equivalent. In our case, the software is based on a strain based periodic homogenization approach involving displacement boundary conditions. This method leads to six linear elasticity problems (1) which have to be solved under strain boundary conditions, such as:  $E_{kh} = 1$  and  $E_{ij} = 0$  if  $(i, j) \neq (k, h)$ .

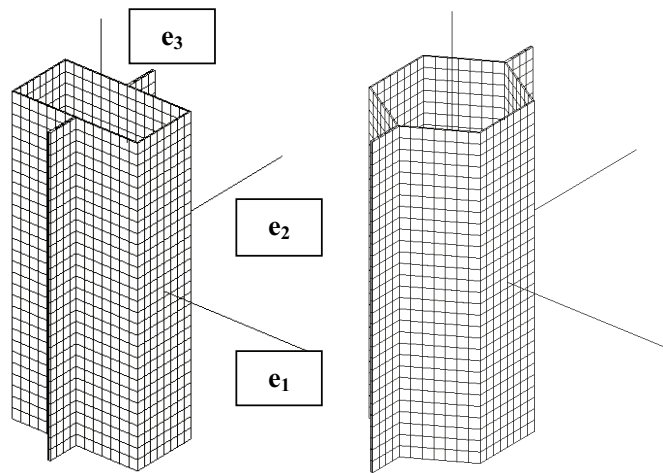


Figure 11: Over-expanded (ECA-R) and hexagonal (ECA-H) honeycomb RVE with orthotropic axis

The six elementary problems to be solved on the RVE  $Y$  are derived hereafter:

$$\begin{aligned}
 \operatorname{div}(\boldsymbol{\sigma}(y)) &= \mathbf{0} \quad \text{in } Y \\
 \boldsymbol{\sigma}(y) &= \mathbf{C}(y)\boldsymbol{\varepsilon}(u(y)) \quad \text{in } Y \\
 \boldsymbol{\varepsilon}(u) &= \operatorname{grad}_s(u(y)) \\
 \boldsymbol{\sigma}(y)\vec{n}_{ext} &= \vec{\mathbf{0}} \quad \text{on } \partial Y_{21} \\
 \vec{u}(y) &= \mathbf{E}\vec{y} + \vec{v}_{per} \quad \text{on } \partial Y_{22}
 \end{aligned} \tag{1}$$

The homogenized mechanical stiffness  $C^{RVE}$  of the RVE can be simply derived with the Hill-Mandel theorem which makes the assumption that the mean energy of the RVE is equal to the energy of the equivalent continuous medium (2):

$$\mathbf{E} : (\mathbf{C}^{RVE} \mathbf{E}) = \frac{1}{|Y|} \int_Y \boldsymbol{\sigma} : \boldsymbol{\varepsilon} dy \tag{2}$$

The anisotropic homogenized elastic stiffness tensor is determined by deriving the twenty one linear combinations of the six elementary problems defined on the RVE. The engineering constants, the Young’s moduli, the Poisson’s ratios and the shear moduli, are deduced from the RVE compliance coefficients.

**Failure Criteria**

Periodic structures typically exhibit many local failures after having been exposed to structural instability. Experimentally it can be observed that the buckling corresponds to a very significant increase in the damage of the walls of the core. During mechanical shear tests or out-of-plane compression tests, a brutal decrease of the load appears after structural instability. This collapse corresponds to the crushing of the walls. Nomex<sup>®</sup> honeycomb cores are known to have a fragile linear elastic mechanical behaviour. In this study, it will be considered that this load corresponds to their ultimate limit. The critical strains are given for the different cases of loadings. The study of the linear elastic buckling of the RVE leads to the identification of the failure stress properties. According to this assumption, Euler’s critical condition then reduces to a standard eigenvalue problem (3). Failure stresses components associated with the critical strains (3) are defined by the equation (4):

$$[\mathbf{K} + \lambda^2 \mathbf{K}_s] \vec{X}_\lambda = \vec{\mathbf{0}} \quad E^c = \lambda^2 E \tag{3}$$

$$\hat{\boldsymbol{\sigma}}_I^c = \hat{\mathbf{C}}_{IJ} \hat{E}_J^c \tag{4}$$

For illustration, the failure envelopes are presented in figures 12, 13 and 14 for combined loadings of compression and shear in the L and W directions, as well as combined shear loadings for ECA-R and ECA-H cores. These ultimate stresses are

determined from the buckling modes of the RVE. The simulations carried out using the NidaCore software are in conformity with the experimental results of Petras and Sutcliffe (2000) obtained from an experimental device ARCAN.

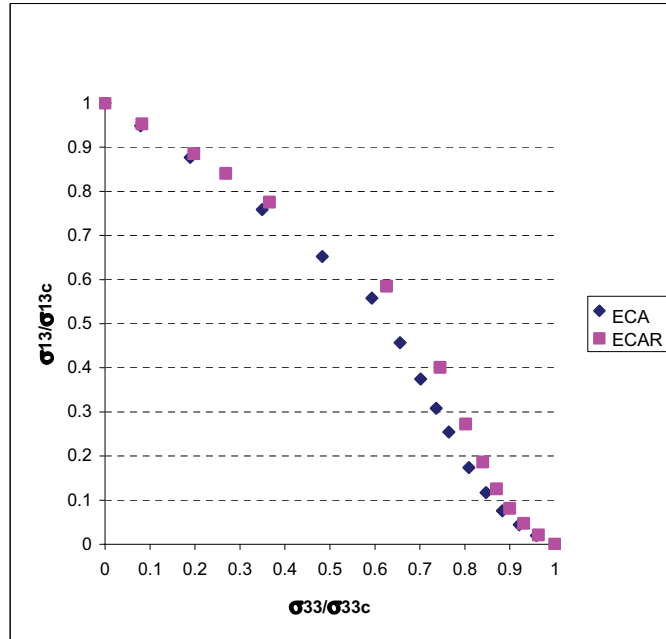


Figure 12:  $\sigma_{13} - \sigma_{33}$  Stress failure predictions for ECA-R  $48 \text{ kg m}^{-3}$  and ECA-H  $48 \text{ kg m}^{-3}$

However, the change of slope observed numerically (figures 12 and 13) is certainly masked in the work of Petras and Sutcliffe (2000) due to the low number of experimental points. According to ECA-H 4.8-48 (51) and ECA-R 4.8-48 (51) numerical failure predictions, we proposed the extended failure envelope as follow:

Failure envelope in the  $\sigma_{13} - \sigma_{23}$  plane:

$$\left(\frac{\sigma_{13}}{\sigma_{13c}}\right)^\alpha + \left(\frac{\sigma_{23}}{\sigma_{23c}}\right)^\alpha = 1 \quad (5)$$

Failure envelope in the  $\sigma_{13} - \sigma_{33}$  plane:

Failure if  $f_{c13-33} = 1$  with  $f_{c13-33} = \min(g_{c13}, f_{c13})$  and

$$g_{c13}(\sigma_{13}, \sigma_{23}) = \left(\frac{\sigma_{13}}{\sigma_{13c}}\right)^{\alpha_{13}} + \left(\frac{\sigma_{23}}{\sigma_{23c}}\right)^{\alpha_{13}} \quad (6)$$

$$f_{c13}(\sigma_{13}, \sigma_{33}) = \gamma_{13} \left(\frac{\sigma_{13}}{\sigma_{13c}}\right)^{\alpha_{13}} + \left(\frac{\sigma_{33}}{\sigma_{33c}}\right)^{\alpha_{13}}$$

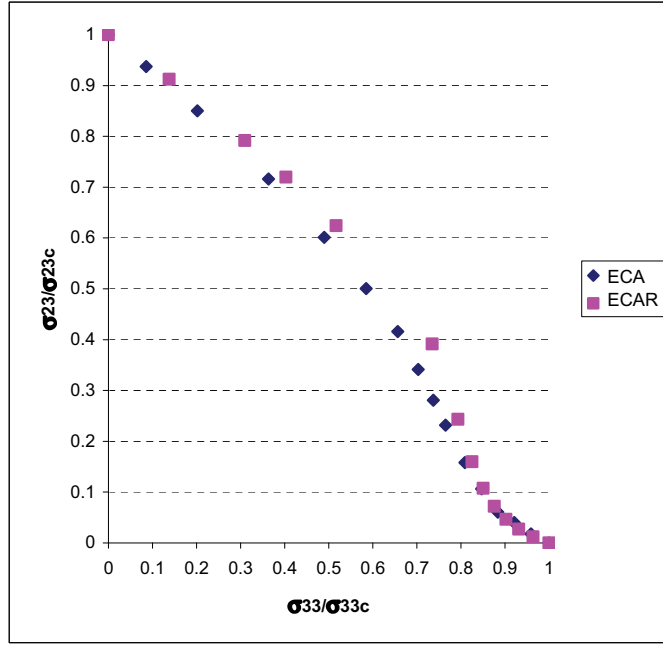


Figure 13:  $\sigma_{23} - \sigma_{33}$  Stress failure predictions for ECA-R  $48 \text{ kg m}^{-3}$  and ECA-H  $48 \text{ kg m}^{-3}$

Failure envelope in the  $\sigma_{23} - \sigma_{33}$  plane:

Failure if  $f_{c23-33} = 1$  with  $f_{c23-33} = \min(g_{c23}, f_{c23})$  and

$$g_{c23}(\sigma_{23}, \sigma_{33}) = \left(\frac{\sigma_{13}}{\sigma_{13c}}\right)^{\alpha_{23}} + \left(\frac{\sigma_{23}}{\sigma_{23c}}\right)^{\alpha_{23}} \quad (7)$$

$$f_{c23}(\sigma_{23}, \sigma_{33}) = \gamma_{23} \left(\frac{\sigma_{23}}{\sigma_{23c}}\right)^{\alpha_{23}} + \left(\frac{\sigma_{33}}{\sigma_{33c}}\right)^{\alpha_{23}}$$

The parameters of the failure criteria are identified to fit the discrete data as illustrated on figures 15 and 16 for combined compression and shear loadings.

The failure envelope could be simplified with linear response but the identification must be conservative with experimental data presented for materials.

$$\begin{aligned} \left(\frac{\sigma_{13}}{\sigma'_{13c}}\right) + \left(\frac{\sigma_{23}}{\sigma'_{23c}}\right) &= 1 \\ \left(\frac{\sigma_{13}}{\sigma'_{13c}}\right) + \left(\frac{\sigma_{33}}{\sigma'_{33c}}\right) &= 1 \\ \left(\frac{\sigma_{13}}{\sigma'_{13c}}\right) + \left(\frac{\sigma_{33}}{\sigma'_{33c}}\right) &= 1 \end{aligned} \quad (8)$$

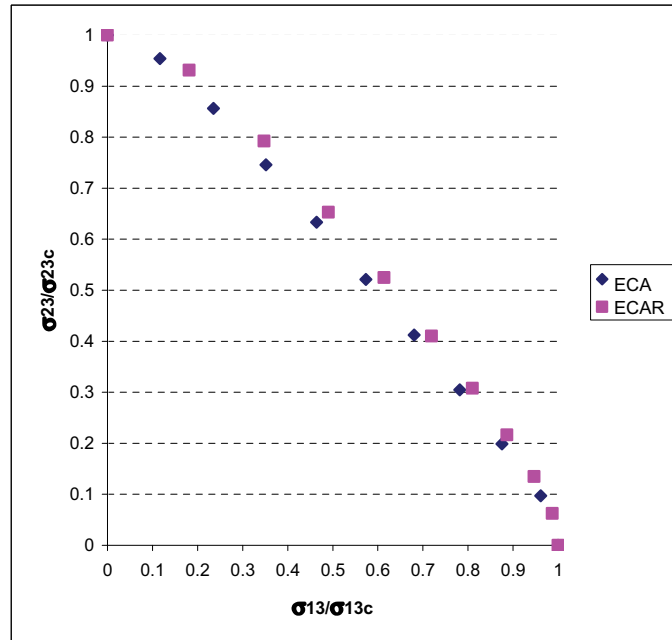


Figure 14:  $\sigma_{23} - \sigma_{13}$  Stress failure predictions for ECAR 48 kg m<sup>-3</sup> and ECA-H 48 kg m<sup>-3</sup>

Table 2: Nomex<sup>®</sup> cores mechanical properties

Material Category Results	ECAR 4.8-48 (51)				ECAR 4.8-48 (51)			
	Minimum		Typical		Minimum		Typical	
	FE	EC	FE	EC	FE	EC	FE	EC
G <sub>23</sub>	34.4	34	41.9	40	19.9	18	25	24
G <sub>13</sub>	22.5	22	27.4	28	34.2	36	42.97	44
G <sub>12</sub>	1.76	-	2.15	-	.71	-	.89	-
E <sub>33</sub>	164.1		199.9		185.6	-	233.6	-
$\sigma_{33c}$	1.3	2.6	1.58	2.85	1.37	2.3	1.72	2.3
$\sigma_{13c}$	.49	.56	.594	.66	0.77	0.72	0.84	0.82
$\sigma_{23c}$	.82	.98	1.003	1.14	0.79	0.66	0.89	0.74

### Conclusion

A canonical base of three mechanical tests associated with finite elements simulations has been proposed to determine all of the three-dimensional quasi-static mechanical properties of the Nomex<sup>®</sup> honeycomb cores. The approach suggested involves four blocks specimens for pure out-of-plane shear tests and standardized specimens for out-of-plane compression tests. Relevance of the mechanical tests, and in particular of the scale effect, is validated using the virtual-sample program. The experimental work carried out in interaction with studies on prototype soft-

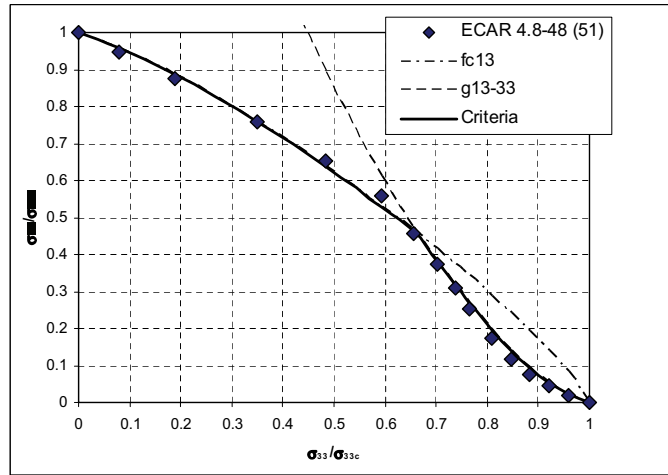


Figure 15:  $\sigma_{13} - \sigma_{33}$  Stress failure criteria for ECA-R 48 kg m<sup>-3</sup>

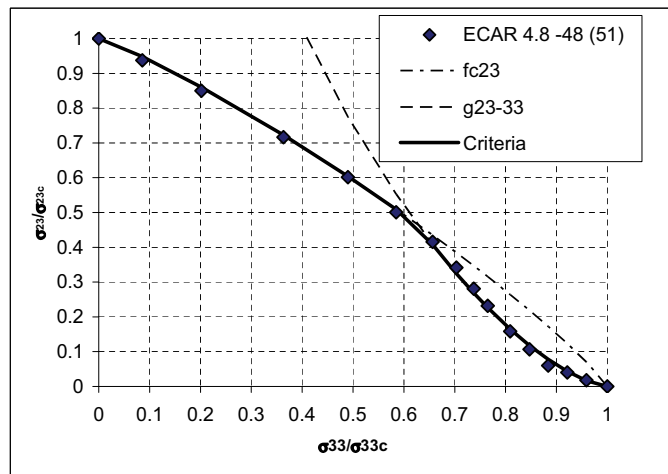


Figure 16:  $\sigma_{23} - \sigma_{33}$  Stress failure criteria for ECA-R 48 kg m<sup>-3</sup>

ware NidaCore, developed from the finite elements code Cast3M-CEA, allows to evaluate the rupture stresses under the action of complex loadings without having to perform additional ARCAN type mechanical tests. A complex failure envelope criterion is proposed. This criterion is identified on the numerical ultimate stresses components given by NidaCore.

### References

1. Aminanda Y., Castanié B., Barrau J-J., Thevenet P., 2005, *Experimental analysis and modelling of the crushing of honeycomb cores*, Applied Composite Materials, pp. 213-227.

2. Euro-Composite 1999, *Nomex<sup>®</sup> cores*, <http://www.euro-composites.com>
3. Gibson L. J., Ashby M.F., 1988, *Cellular Solids Structures and Properties*, Pergamon Press, Oxford.
4. Gornet L., Marckmann G., Lombard M., 2004, *Détermination des coefficients d'élasticité et de rupture d'âmes nids d'abeilles Nomex<sup>®</sup>: homogénéisation périodique et simulation numérique*, Mécanique Industrie, pp. 595-604.
5. Gornet L., Marguet S., Marckmann G., 2006, *Failure criteria and effective elastic properties of Nomex<sup>®</sup> honeycomb cores: modelling and experimental validation*, International Journal Computer Material & Continua, Tech Science Press, 4, 2.
6. Hexcel 1999, *HexWebTB Honeycomb Attributes and properties*, Hexcel Composites
7. Martin F, Alesandrini B., Gornet L., Markmann G., Roland P., Gilles Ollier Design Team, 2006 *Conception d'un grand multicoque de course au Large : l'exemple d'Orange II.*, Association Technique Maritime et Aéronautique.
8. Petras A, Sutcliffe, 1999, *Failure Mode Maps for Honeycomb Sandwich panels*, Composite Structures, 44, pp. 237-252.
9. Petras A, Sutcliffe, 2000, *Indentation failure analysis of sandwich beams*, Composite Structures, 30, pp. 311-318.
10. Zhang J., M.F. Ashby, 1992, *The out-of-plane properties of honeycombs*, International Journal of Mechanical Sciences, 35 (5) pp. 475-489.